

NASA Technical Memorandum 80174

(NASA-TM-80174) STRESS-INTENSITY FACTORS
AND CRACK-OPENING DISPLACEMENTS FOR ROUND
COMPACT SPECIMENS (NASA) 30 p HC A93/MF A01
CSCL 20K

N80-15430

Unclas
G3/39 46627

STRESS-INTENSITY FACTORS AND CRACK-OPENING
DISPLACEMENTS FOR ROUND COMPACT SPECIMENS

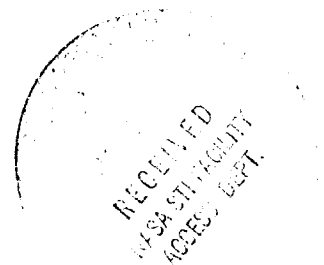
J. C. Newman, Jr.

OCTOBER 1979

NASA

National Aeronautics and
Space Administration

Langley Research Center
Hampton, Virginia 23665



STRESS-INTENSITY FACTORS AND CRACK-OPENING DISPLACEMENTS

FOR ROUND COMPACT SPECIMENS

J. C. Newman, Jr.
NASA Langley Research Center
Hampton, Virginia 23665

ABSTRACT

A two-dimensional, boundary-collocation stress analysis was used to analyze various round compact specimens. The influence of the round external boundary and of pin-loaded holes on stress-intensity factors and crack-opening displacements was determined as a function of crack-length-to-specimen-width ratios. A wide-range equation for the stress-intensity factors, like that developed for the "standard" rectangular compact specimen, was developed. Equations for crack-surface displacements and load-point displacements were also developed.

In addition, stress-intensity factors were calculated from compliance methods to demonstrate that load-displacement records must be made at the loading points and not along the crack line (as is customary) for crack-length-to-specimen-width ratios less than about 0.4.

INTRODUCTION

The round compact specimen, an edge-cracked disk shown in figure 1, is currently being considered for incorporation into ASTM Standard Test Method for Plane Strain Fracture Toughness of Metallic Materials (ASTM E399). The round compact specimen is a convenient configuration for testing of materials cut from round bars, and it is cheaper to machine than the "standard" rectangular compact specimen.

In 1973, Feddern and Mackerauch [1] proposed a round compact specimen for fracture-toughness testing. Later, Mowbray and Andrews [2], Cull and Starrett [3], and James and Mills [4] used a similar round compact specimen to test for fracture toughness and fatigue crack growth rates. Table I shows the chronological development and a comparison of dimensions for the various round compact specimens that have been tested or analyzed. The earlier round compact specimens had hole sizes and locations that were different from the standard compact specimen. As shown in figure 2, the proposed ASTM round compact specimen design (solid lines) conforms closely to that of the standard rectangular compact specimen (dashed lines). In fact, because the hole size and locations are the same for both specimens, the same loading fixtures can be used.

Stress-intensity factors and crack-surface displacements for round compact specimens without pin-loaded holes have been obtained previously from boundary-collocation analyses by Gross [5] and from closed-form asymptotic solutions by Gregory [6]. For specimens with pin-loaded holes, finite-element models [2] have been used, but the analyst considered only a limited range of crack lengths. Stress-intensity factors have also been determined from experimental compliance measurements [1] for a limited range of crack lengths.

In the present paper, an improved method of boundary collocation [7,8] was applied to the two-dimensional stress analysis of round compact specimens with pin-loaded holes. The method was based on the complex variable analysis of Muskhelishvili [9]. The complex-series stress functions developed in reference 8 were constructed so that the governing equations of elasticity and the boundary conditions on the crack surfaces were satisfied exactly, while the

boundary conditions on the external boundary and the pin-loaded holes were satisfied approximately. In contrast to previous collocation methods in which the boundary stresses were specified, the collocation method used herein requires that the resultant forces on the boundaries be specified (in a least-squares sense). The improved method was shown [7] to converge more rapidly than previously used collocation methods.

By using the improved method, stress-intensity factors and crack-opening displacements for various round compact specimens were calculated as a function of crack-length-to-specimen-width ratios. A "wide-range" equation for the stress-intensity factors, like that developed for the standard rectangular compact specimen [10], was developed. Equations for crack-surface displacements and load-point displacements were also developed.

SYMBOLS

a	distance from centerline of applied load to crack tip
c	crack length measured from the edge of the disk
D	diameter of round compact specimen
d	distance from the plane of the crack to the center of the circular hole
E	Young's modulus
K	stress-intensity factor (mode I)
L	distance measured from center of disk to load line (see fig. 2)
N_T	total number of coefficients used in collocation analysis
P	load per unit thickness acting in the y-direction
R	radius of the circular holes
v_0, v_1, v_2	crack-surface displacements in y-direction (see fig. 2)
v_3	displacement at point of load application in y-direction (see fig. 2)

W	"width" of round specimen measured from centerline of applied load
κ	material constant, $\kappa = 3 - 4\nu$ for plane strain and $\kappa = \frac{3 - \nu}{1 + \nu}$ for generalized plane stress
ν	Poisson's ratio
σ_n	normal stress at boundary of hole

ANALYSIS OF THE ROUND COMPACT SPECIMEN

This analysis was identical to that developed previously for the rectangular compact specimen [8] except that the external boundary was made circular. The details of the analysis are given in reference 8 and are not repeated here. The analysis was applied herein to three different round compact specimen configurations. The three configurations analyzed were: (1) the Feddern-Macherauch round compact specimen design, (2) the proposed ASTM round compact specimen (denoted herein as type I), and (3) the proposed ASTM round compact specimen with a flat section at the crack mouth (type II). The type I and II specimens are shown in figure 2. The type I specimen is fully round and the type II specimen has a flat section at the crack mouth (crosshatched area removed). The flat section corresponds exactly to that in the standard compact specimen (dashed lines). In figure 2, the locations 0, 1, 2, and 3 indicate the points at which the crack-opening displacements (V_0 , V_1 , V_2 , and V_3) were calculated.

Loading

All round compact specimens were analyzed with simulated pin loading in the holes. For simplicity, a uniform radial stress, σ_n , was assumed to apply on the hole boundaries over a total arc of 40 degrees. This pin-load simulation was used for two reasons. First, in the actual specimens, the bearing stresses on the boundary of the holes caused by the pin loading

are concentrated over a small arc due to the undersized pin requirements in ASTM E399-78. Second, reference 8 has shown that the stress-intensity factors and crack-surface displacements for the standard rectangular compact specimen with $a/W \geq 0.2$ are not influenced by the particular stress distribution applied on the hole boundary.

Convergence

Because boundary collocation is a numerical method, convergence of the solution must be investigated. Convergence was studied for several a/W ratios (0.2, 0.5, and 0.8) using several values of N_T , the total number of coefficients in the series stress functions [8]. The configurations with $a/W = 0.2$ and 0.8 were selected because the close proximity of the crack tip to the holes and external boundary, respectively, were expected to pose convergence difficulties. In figure 3, the stress-intensity factors are plotted as functions of N_T . For ease of comparison, the stress-intensity factors are normalized with respect to their value for $N_T = 160$ (the largest value considered). As the number of terms in the series was increased, the differences between the specified boundary conditions and those obtained from the series solution became smaller and the stress-intensity ratio converged to unity. The convergence was satisfactory at $N_T = 160$ for all a/W ratios considered. Thus, for all other configurations investigated, 150 coefficients were used.

Effects of κ on Stress-Intensity Factors

Stress-intensity factors for cracked specimens with internal loading (such as pin loading) are functions of Poisson's ratio and the plane-stress or plane-strain assumption. Both of these effects on stress-intensity factors

can be studied by considering variations in κ only. The type I configuration was analyzed for several values of κ . The results indicated that variations in κ (hence, plane-stress or plane-strain assumptions) had an extremely small effect on stress intensity. For example, for an a/W ratio of 0.2 the stress-intensity factor varied by less than 0.5 percent for κ between 1 and 3. The effects of κ on stress-intensity factors were even smaller for larger values of a/W .

RESULTS AND DISCUSSION

In the following sections, stress-intensity factors and crack-opening displacements for various round compact specimens are presented. All specimen configurations were subjected to simulated pin loading in the holes. A wide-range stress-intensity factor equation was developed for the proposed ASTM round compact specimens. Equations for crack-surface and load-point displacements were also developed.

Stress-Intensity Factors

Feddern-Macherauch round compact specimen.- The stress-intensity factors calculated from the present method and from Gross [5] for the Feddern-Macherauch specimen ($D/W = 1.333$) are shown in table II for various a/W ratios. Gross analyzed a configuration that did not include the pin-loaded holes, but used shear forces along the load line to simulate pin loading. For an a/W ratio of 0.2, the percentage difference between the two solutions is about 16 percent. This difference is attributed to the influence of the pin-loaded holes. Similar differences were observed for the standard rectangular compact specimen with [8] and without [11] the pin-loaded holes and are also shown in table II.

Proposed ASTM round compact specimens.- The stress-intensity factors calculated from the present method for the proposed ASTM specimens (types I and II) are given in table III for various a/W ratios and are compared with other stress-intensity factor solutions for fully round compact specimens. Gross [5] obtained a collocation solution and Gregory [6] obtained a closed-form asymptotic solution for configurations that did not include pin-loaded holes. The results from Gross and Gregory, which are in good agreement with each other, are about 15-percent higher than the present solutions for short crack lengths ($a/W = 0.2$). Their high values were due to neglecting the influence of the pin-loaded holes. Mowbray and Andrews [2] used the finite-element method. Feddern and Macherauch [1] used experimental load-line (crack surface) displacements and the compliance method to obtain stress-intensity factors. In the appendix, load-line (V_2) and load-point (V_3) displacements were calculated to demonstrate that displacements must be measured at the loading points, and not along the crack surface, to obtain accurate stress-intensity factors for a/W ratios less than about 0.4. As shown in table III, all solutions are in good agreement for a/W ratios greater than 0.4.

Wide-range stress-intensity factor equation.- The present results and those in reference 8 indicate that for compact specimens the pin-loaded holes have a significant influence on stress-intensity factors for a/W ratios less than 0.4. Therefore, when the round specimen is used at a/W ratios less than 0.4 the effects of the holes should be included. A wide-range equation, like that developed for the standard rectangular compact specimen [10], was chosen to fit the present results. The equation was

$$K = \frac{P}{\sqrt{W}} \frac{(2 + \lambda)}{\sqrt{(1 - \lambda)^3}} G \quad (1)$$

where $\lambda = a/W$ and

$$G = 0.76 + 4.8\lambda - 11.58\lambda^2 + 11.43\lambda^3 - 4.08\lambda^4 \quad (2)$$

for $0.2 \leq \lambda < 1$. Equation (2) is a least-squares fit to the present results. Equation (1) agrees to within 0.3 percent of the present results given in table III for the type I and II round compact specimens. Equation (1) also approaches the exact asymptotic solution as λ approaches unity [6,12].

Comparison of round and rectangular compact specimens.- The nondimensional stress-intensity factors from the present collocation results are plotted as symbols in figure 4. The solid curve shows the results of equation (1) for the round compact specimens (types I and II). The dashed curve shows the wide-range equation developed by Srawley [10] for the rectangular compact specimen. For $a/W = 0.2$, the stress-intensity factors for the round specimen are about 4-percent lower than those from the rectangular specimen. But for a/W ratios between 0.4 and 0.7, the stress-intensity factors from the round specimen are about 6-percent higher than those from the rectangular specimen. For large crack lengths ($a/W > 0.8$), the stress-intensity factors approach each other.

Crack-Opening Displacements

Crack-opening displacements are functions of Poisson's ratio and of whether plane stress or plane strain is assumed. Because experimental displacements agree well with calculated displacements under plane-stress conditions for rectangular compact specimens [8], all calculations herein were made with $\nu = 2.077$ (Poisson's ratio of 0.3 under plane-stress conditions).

Figure 5 shows the nondimensional crack-surface displacements, EV/P , at various locations along the crack line for round compact specimens (types I

and II) as a function of a/W . V_0 and V_1 are the crack-mouth displacements for type I and II specimens, respectively, and V_2 is the load-line displacements for both specimens. The load-line displacements, V_2 , are nearly the same for both specimens. The V_1 displacements for type II are slightly higher than those for type I.

Table IV presents the nondimensional crack-opening displacements, EV/P , at various locations along the crack line and at the load point for the round and rectangular compact specimens as a function of a/W .

For ease of computation, polynomial expressions for the crack-surface and load-point displacements were developed for round and rectangular compact specimens. The polynomial expression is

$$\ln \frac{EV}{P} = \sum_{j=1}^5 A_j \left(\frac{a}{W}\right)^{j-1} \quad (3)$$

The solid and dashed curves in figure 5 show the displacements calculated from the polynomial expression fitted (by least squares) to the present collocation results for type I and II round specimens, respectively. The coefficients A_j are given in table V for various locations along the crack line and at the load point for round and rectangular compact specimens. The polynomial expressions were within 0.5 percent of the collocation results for $0.2 \leq a/W \leq 0.8$.

In table VI, the crack-opening displacements, EV/P , at the crack mouth, the load line (crack surface), and the load point, from the present results, are compared with experimental results from Fisher and Buzzard [13] for the proposed round specimen (type II). The present results are generally within ± 3 percent of the experimental displacements.

CONCLUDING REMARKS

An improved method of boundary collocation, which accounted for the influence of the pin-loaded holes, was employed in the two-dimensional stress analysis of round compact specimens. The influence of the round external boundary and the pin-loaded holes on stress-intensity factors and crack-opening displacements were investigated for crack-length-to-specimen-width ratios (a/W) ranging from 0.2 to 0.8.

The stress-intensity factors calculated from the present method for a/W ratios less than 0.4 were lower than those computed from analyses that did not include the pin-loaded holes--as much as 15 percent for $a/W = 0.2$. But the stress-intensity factors were in good agreement with other solutions from the literature for a/W ratios greater than 0.4. An empirical equation for stress-intensity factors was developed which accounts for the influence of the pin-loaded holes and applies over a wide range of a/W (0.2 to 1). In the appendix, stress-intensity factors were also calculated from compliance methods to demonstrate that load-displacement records must be made at the loading points to give the correct energy-release rate and not along the crack line (as is customary) for a/W ratios less than about 0.4.

The crack-opening displacements calculated from the present method at the crack mouth, load line (crack surface), and load point of the round compact specimen under plane-stress conditions were generally within ± 3 percent of experimental measurements. Accurate polynomial expressions were also developed for the crack-opening displacements at various locations along the crack line and the load point for round and rectangular compact specimens. The polynomial expressions were within ± 0.5 percent of the collocation results for $0.2 \leq a/W \leq 0.8$.

APPENDIX

DETERMINATION OF STRESS-INTENSITY FACTORS FROM COMPLIANCE METHOD

The compliance method is often used to experimentally determine stress-intensity factors from load-displacement records. To obtain accurate stress-intensity factors from compliance measurements, the displacements must be measured at the load points to give the correct energy-release rate from theory of elasticity. However, for convenience a number of investigators have used crack-surface displacements along the load line (such as the V_2 displacement in fig. 2) instead of at the load points. Figure 6 shows that the load-point displacements, V_3 , are considerably larger than the load-line displacements, V_2 , for small values of a/W . The displacements and the compliance relationship [14] were then used to calculate stress-intensity factors as

$$K = \sqrt{EP \frac{dV}{da}} \quad (A1)$$

for plane stress.

In the present paper the slope, dV/da , was approximated by solving for displacements for two crack lengths ($a - \Delta a$ and $a + \Delta a$) as

$$\frac{dV}{da} \approx \frac{V_j(a - \Delta a) - V_j(a + \Delta a)}{2 \Delta a} \quad (A2)$$

where $V_j(\)$ was the displacement for the specified crack length with $j = 2$ or 3, and the incremental change in crack length, Δa , was $0.001W$.

Table VII shows the normalized stress-intensity factors for the round compact specimen (type I) determined by collocation using either stress functions or compliance. The values from compliance were determined using either the calculated load-point displacements or the calculated load-line displacements.

The stress-intensity factors computed from the load-point displacements were in excellent agreement with the collocation (stress function) values, whereas the values computed from the load-line displacements were in considerable disagreement for a/W ratios less than 0.4.

REFERENCES

1. Feddern, G. V.; and Macherlauch, E.: A New Specimen Geometry for K_{Ic} - Measurements. *Z. Metallkde*, vol. 64, 1973, pp. 882-884.
2. Mowbray, D. F.; and Andrews, W. R.: Stress-Intensity Factor Calibration for a Compact Specimen with a Round Profile. General Electric Technical Information Series No. 74SL235, 1975.
3. Cull, A. D.; and Starrett, H. S.: A Study of Fracture Mechanics for Graphite Materials. AFML-TR-75-125, Air Force Materials Laboratory, 1975.
4. James, L. A.; and Mills, W. J.: An Evaluation of the Round Compact Specimen for Fatigue-Crack Growth Rate Testing. HEDL-TME 78-56, Hanford Engineering Development Laboratory, 1978.
5. Gross, B.: Mode I Analysis of a Cracked Circular Disk Subject to a Couple and a Force. NASA TM X-73692, 1977.
6. Gregory, R. D.: The Edge-Cracked Circular Disc Under Symmetric Pin-Loading. Technical Report No. 78-36, The University of British Columbia, Vancouver, 1978.
7. Newman, J. C., Jr.: An Improved Method of Collocation for the Stress Analysis of Cracked Plates with Various Shaped Boundaries. NASA TN D-6376, 1971.
8. Newman, J. C., Jr.: Stress Analysis of the Compact Specimen Including the Effects of Pin Loading. Fracture Analysis, ASTM STP-560, American Society for Testing and Materials, 1974, pp. 105-121.
9. Muskhelishvili, N. I. (J. R. M. Radok, transl.): Some Basic Problems of the Mathematical Theory of Elasticity. Third ed. P. Noordhoff, Ltd., 1953.
10. Srawley, J. E.: Wide Range Stress Intensity Factor Expressions for ASTM E399 Standard Fracture Toughness Specimens. *International J. of Fracture Mechs.*, vol. 12, June 1976, pp. 475-476.
11. Srawley, J. E.; and Gross, B.: Stress-Intensity Factors for Bend and Compact Specimens. *Engr. Fracture Mechs. J.*, vol. 4, no. 3, September 1972, pp. 587-589.
12. Bentham, J. T.; and Koiter, W. T.: Asymptotic Approximations to Crack Problems. *Mechanics of Fracture I - Methods of Analysis and Solution of Crack Problems*, Noordhoff International Publications, 1973, pp. 159-162.
13. Fisher, D. M.; and Buzzard, R. J.: Comparison Tests and Experimental Compliance Calibration of the Proposed Standard Round Compact Plane Strain Fracture Toughness Specimen. NASA TM-81379, 1979.
14. Paris, P. C.; and Sih, G. C.: Stress Analysis of Cracks. *Fracture Toughness Testing and Its Applications*, ASTM STP-381, American Society for Testing and Materials, 1964, pp. 30-81.

TABLE I.- CHRONOLOGICAL DEVELOPMENT OF ROUND COMPACT SPECIMENS

Reference	Date	L/W	D/W	Hole Location	
				d/W	R/W
Feddern and Macherauch [1]	1973	0.333	1.333 (ε)	0.266	0.133
Mowbray and Andrews [2]	1975	0.333	1.333 (a)	0.333	0.083
Cull and Starrett [3]	1975	0.333	1.333 (a)	0.250	0.083
Gross [5]	1977	0.333	1.333 (a)	No hole	No hole
Gregory [6]	1978	Various	Various	No hole	No hole
Proposed (ASTM)	1978	0.325	1.35	0.275 (b)	0.125 (b)

(a) $D/W = 1.333$ for load line at $L = D/4$ (see fig. 2).

(b) Dimensions are identical to those in standard compact specimen.

TABLE II.- COMPARISON OF NORMALIZED STRESS-INTENSITY FACTOR, $K\sqrt{W}/P$, FOR ROUND AND RECTANGULAR COMPACT SPECIMENS WITH AND WITHOUT PIN-LOADED HOLES

a/W	Round Compact (a)				Rectangular Compact (b)		
	Gross [5] (c)	Present Results (d)	Percent Difference	Strawley-Gross [11] (c)	Newman [8] (d)	Percent Difference	
0.2	4.74	4.08	16.2	4.75	4.29	10.7	
0.3	--	5.63	--	5.84	5.63	3.7	
0.4	7.61	7.52	1.2	7.33	7.27	0.8	
0.5	--	10.19	--	9.63	9.63	0	
0.6	14.53	14.55	-0.1	13.62	13.64	-0.1	
0.7	--	22.84	--	21.56	21.57	0	
0.8	42.77	42.79	0.0	41.07	41.13	-0.1	

(a) Feddern-Macherauch round compact specimen design (D/W = 1.333).

(b) Standard rectangular compact specimen design (ASTM E399).

(c) Specimen configuration without pin-loaded hole.

(d) Specimen configuration with pin-loaded hole.

TABLE III.- COMPARISON OF NORMALIZED STRESS-INTENSITY FACTOR, $K\sqrt{a}/P$ FOR THE

VARIOUS ROUND COMPACT SPECIMENS

a/w	Present Results D/W = 1.35		Gregory [6] (a) D/W = 1.35	Gross [5] (b) D/W = 1.333	Mowbray and Andrews [2] (c) D/W = 1.333	Feddern and Macherauch [1] (d) D/W = 1.333
	Type I	Type II				
0.20	4.138	4.115	4.781	4.745	--	--
0.25	4.853	4.839	5.301	--	--	--
0.30	5.636	5.629	5.924	--	--	5.865
0.35	6.506	6.503	6.68	--	--	--
0.40	7.505	7.506	7.60	7.61	--	7.30
0.45	8.697	8.700	8.74	--	--	--
0.50	10.17	10.17	10.18	--	10.18	10.02
0.55	12.05	12.05	12.04	--	--	--
0.60	14.52	14.53	14.51	14.53	14.73	14.72
0.65	17.92	17.93	17.91	--	--	--
0.70	22.81	22.82	22.80	--	22.65	22.94
0.75	30.28	30.29	30.27	--	--	--
0.80	42.75	42.76	42.73	42.77	42.52	--

(a) Asymptotic analysis without pin-loaded hole.

(b) Collocation analysis without pin-loaded hole.

(c) Finite-element analysis with pin-loaded hole.

(d) Experimental-compliance method.

TABLE IV.- NORMALIZED CRACK-SURFACE AND LOAD-POINT DISPLACEMENTS, EV/P , FOR ROUND AND RECTANGULAR COMPACT SPECIMENS (PLANE STRESS WITH $\nu = 0.3$)

a/w	Round Compact												Rectangular Compact		
	Type I						Type II						EV_1/P	EV_2/P	EV_3/P
	EV_0/P	EV_1/P	EV_2/P	EV_3/P	EV_1/P	EV_2/P	EV_3/P	EV_1/P	EV_2/P	EV_3/P	EV_1/P	EV_2/P			
0.20	8.768	7.571	3.909	7.014	7.973	3.899	7.091	8.851	4.277	7.417	8.851	4.277	7.417		
0.25	10.46	9.130	5.161	8.024	9.503	5.148	8.093	10.45	5.564	8.473	10.45	5.564	8.473		
0.30	12.65	11.13	6.708	9.399	11.48	6.693	9.462	12.45	7.111	9.861	12.45	7.111	9.861		
0.35	15.47	13.69	8.662	11.24	14.03	8.645	11.30	14.94	9.013	11.66	14.94	9.013	11.66		
0.40	19.13	17.02	11.18	13.69	17.35	11.16	13.74	18.08	11.40	13.99	18.08	11.40	13.99		
0.45	23.93	21.39	14.48	16.96	21.71	14.47	17.01	22.11	14.45	17.01	22.11	14.45	17.01		
0.50	30.34	27.24	18.92	21.39	27.56	18.91	21.45	27.37	18.46	21.02	27.37	18.46	21.02		
0.55	39.14	35.28	25.06	27.52	35.60	25.04	27.59	34.49	23.92	26.47	34.49	23.92	26.47		
0.60	51.60	46.68	33.81	36.29	47.01	33.80	36.36	44.51	31.64	34.21	44.51	31.64	34.21		
0.65	70.01	63.55	46.84	49.35	63.89	46.84	49.42	59.34	43.14	45.72	59.34	43.14	45.72		
0.70	98.74	89.93	67.34	69.86	90.28	67.34	69.94	82.74	61.37	63.97	82.74	61.37	63.97		
0.75	147.0	134.3	102.0	104.6	134.7	102.0	104.7	122.7	92.68	95.29	122.7	92.68	95.29		
0.80	237.2	217.4	167.2	169.8	217.8	167.3	169.9	197.5	151.5	154.1	197.5	151.5	154.1		

TABLE V.- COEFFICIENTS FOR NORMALIZED CRACK-OPENING DISPLACEMENT EQUATION (a) FOR ROUND AND RECTANGULAR COMPACT SPECIMENS (PLANE STRESS WITH $\nu = 0.3$)

A _j	Round Compact										Rectangular Compact		
	Type I					Type II							
	EV ₀ /P	EV ₁ /P	EV ₂ /P	EV ₃ /P	EV ₁ /P	EV ₂ /P	EV ₃ /P	EV ₁ /P	EV ₂ /P	EV ₃ /P	EV ₁ /P	EV ₂ /P	EV ₃ /P
A ₁	1.829	1.607	0.256	1.931	1.742	0.26	1.96	1.8	0.359	1.905			
A ₂	-0.451	0.117	5.453	-2.889	-0.495	5.381	-3.02	0.122	5.574	-2.098			
A ₃	14.73	13.52	1.841	19.59	14.71	2.105	19.83	12.49	0.836	17.45			
A ₄	-22.26	-20.94	-8.485	-26.63	-22.06	-8.853	-26.83	-20.7	-8.271	-25.66			
A ₅	14.57	14.03	8.944	16.14	14.44	9.122	16.2	14.63	9.521	16.55			

(a) $\lambda_n \frac{EV}{P} = \sum_{j=1}^5 A_j \left(\frac{a}{W}\right)^{j-1}$; $0.2 \leq \frac{a}{W} \leq 0.8$.

TABLE VI.- COMPARISON OF THEORETICAL AND EXPERIMENTAL NORMALIZED CRACK-SURFACE AND LOAD-POINT DISPLACEMENTS, EV_1/P , FOR THE ROUND COMPACT SPECIMEN (TYPE II)

a/W	Crack Mouth, EV_1/P			Load Line, EV_2/P			Load Point, EV_3/P		
	Exp (a)	Theory (b)	Percent Difference	Exp (a)	Theory (b)	Percent Difference	Exp (a)	Theory (b)	Percent Difference
0.2	8.065	7.973	1.1	4.02	3.899	3.1	6.765	7.091	-4.6
0.3	11.55	11.48	0.6	6.77	6.693	1.1	9.18	9.462	-3.0
0.4	17.49	17.35	0.8	11.18	11.16	0.2	13.45	13.74	-2.1
0.5	27.76	27.56	0.7	19.18	18.91	1.4	21.22	21.45	-1.1
0.6	46.60	47.01	-0.9	33.66	33.80	-0.4	36.29	36.36	-0.2
0.7	89.78	90.28	-0.6	67.37	67.34	-0.1	70.00	69.94	0.1
0.8	216.3	217.8	-0.7	165.3	167.3	1.2	169.00	169.9	-0.5

(a) NASA-Lewis experimental data, Fisher and Buzzard [13].

(b) Present collocation results (plane stress with $\nu = 0.3$).

TABLE VII.- NORMALIZED STRESS-INTENSITY FACTOR, $K\sqrt{a}/P$, COMPUTED FROM COLLOCATION AND COMPLIANCE METHOD USING LOAD-POINT AND LOAD-LINE DISPLACEMENTS FROM THE ROUND COMPACT SPECIMEN (TYPE I)

a/w	Collocation-Stress Functions	Collocation-Compliance			Percent Error
		Load Point, V_3	Load Line, V_2		
0.2	4.138	4.139	4.762		15
0.3	5.636	5.636	5.800		4
0.4	7.505	7.504	7.569		1
0.5	10.168	10.167	10.169		0
0.6	14.524	14.523	14.511		0
0.7	22.812	22.809	22.800		0
0.8	42.749	42.750	42.746		0

REF. BY OF THE
ORIGINAL PAGE IS POOR

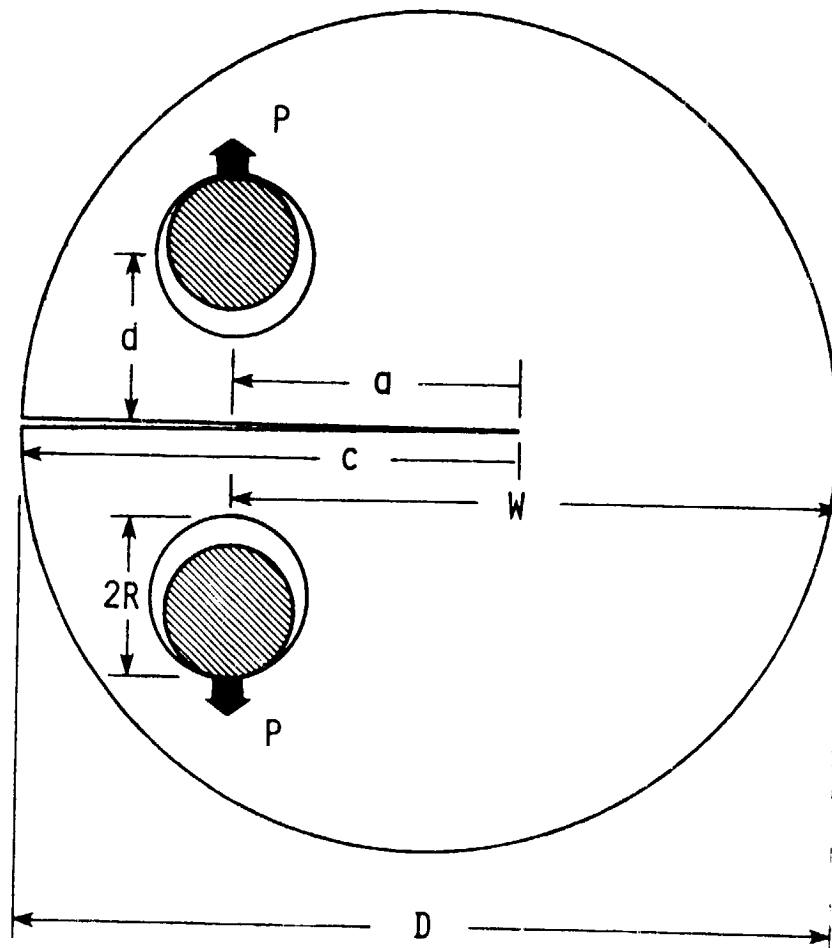


Figure 1.- Round compact specimen subjected to pin loading.

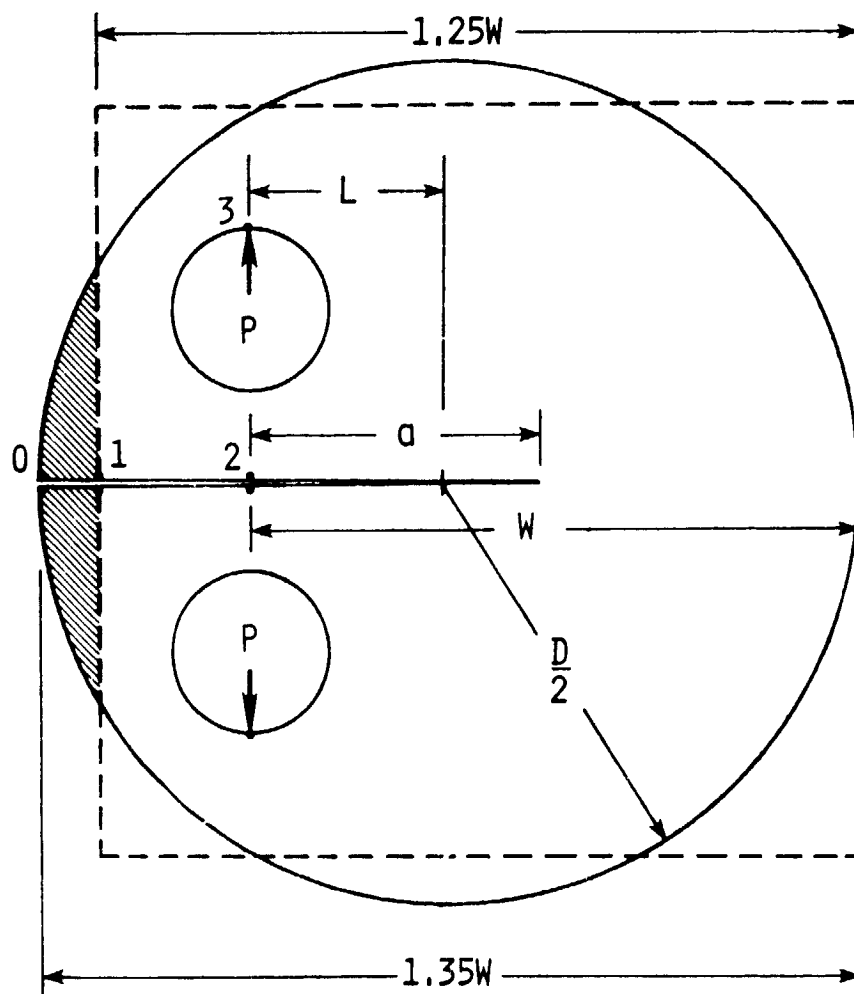


Figure 2.- Type I (fully round) and type II (with flat) round compact specimens and rectangular compact specimen (dashed lines).

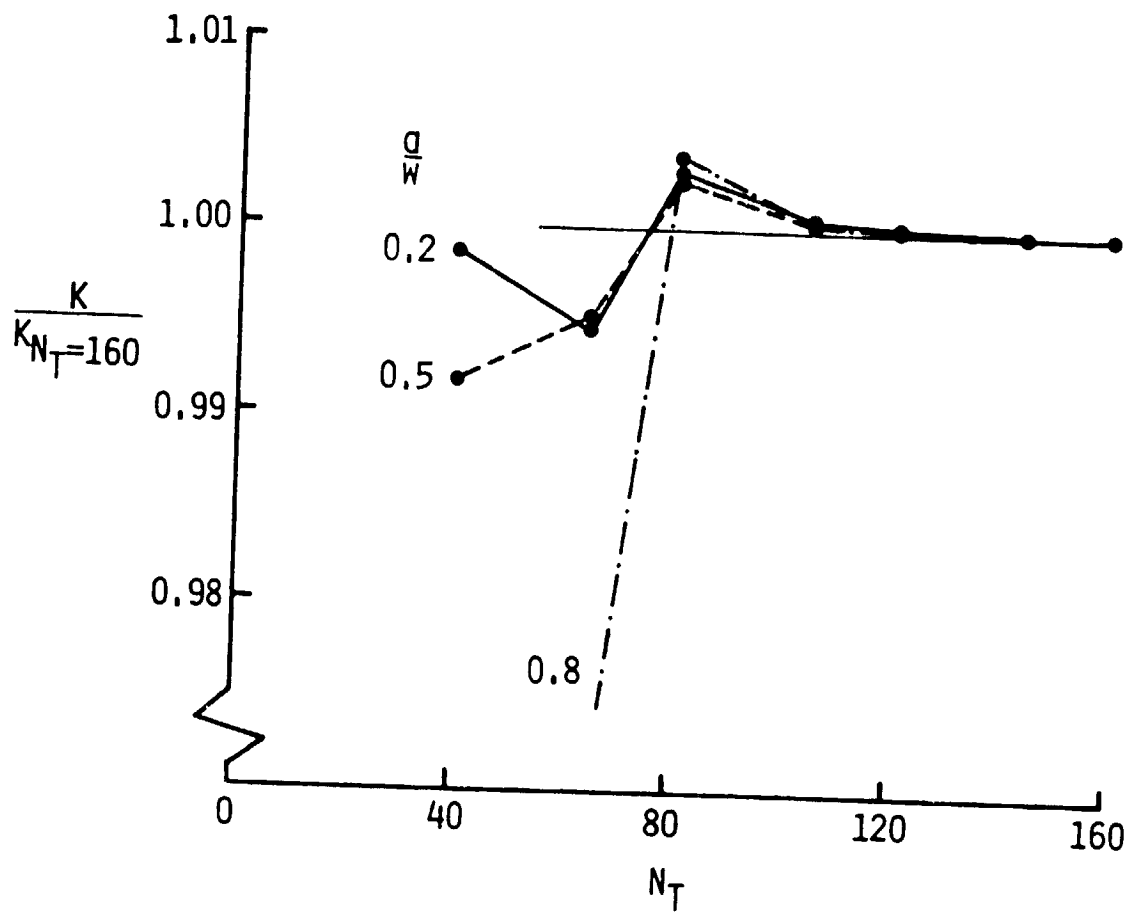


Figure 3.- Convergence of stress-intensity factors for round compact specimen (type I) as a function of number of coefficients.

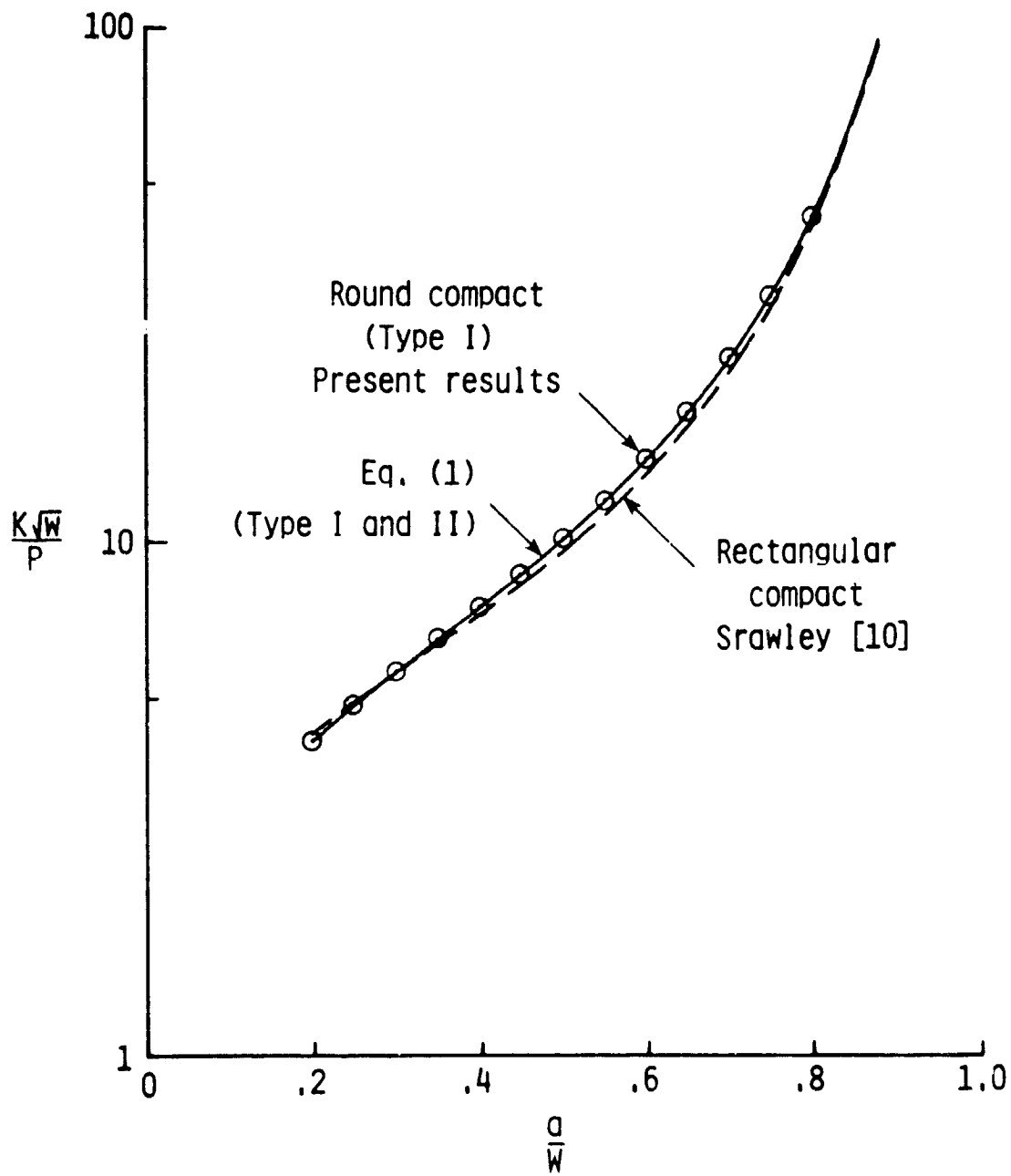


Figure 4.- Normalized stress-intensity factors for round and rectangular compact specimens as a function of a/W .

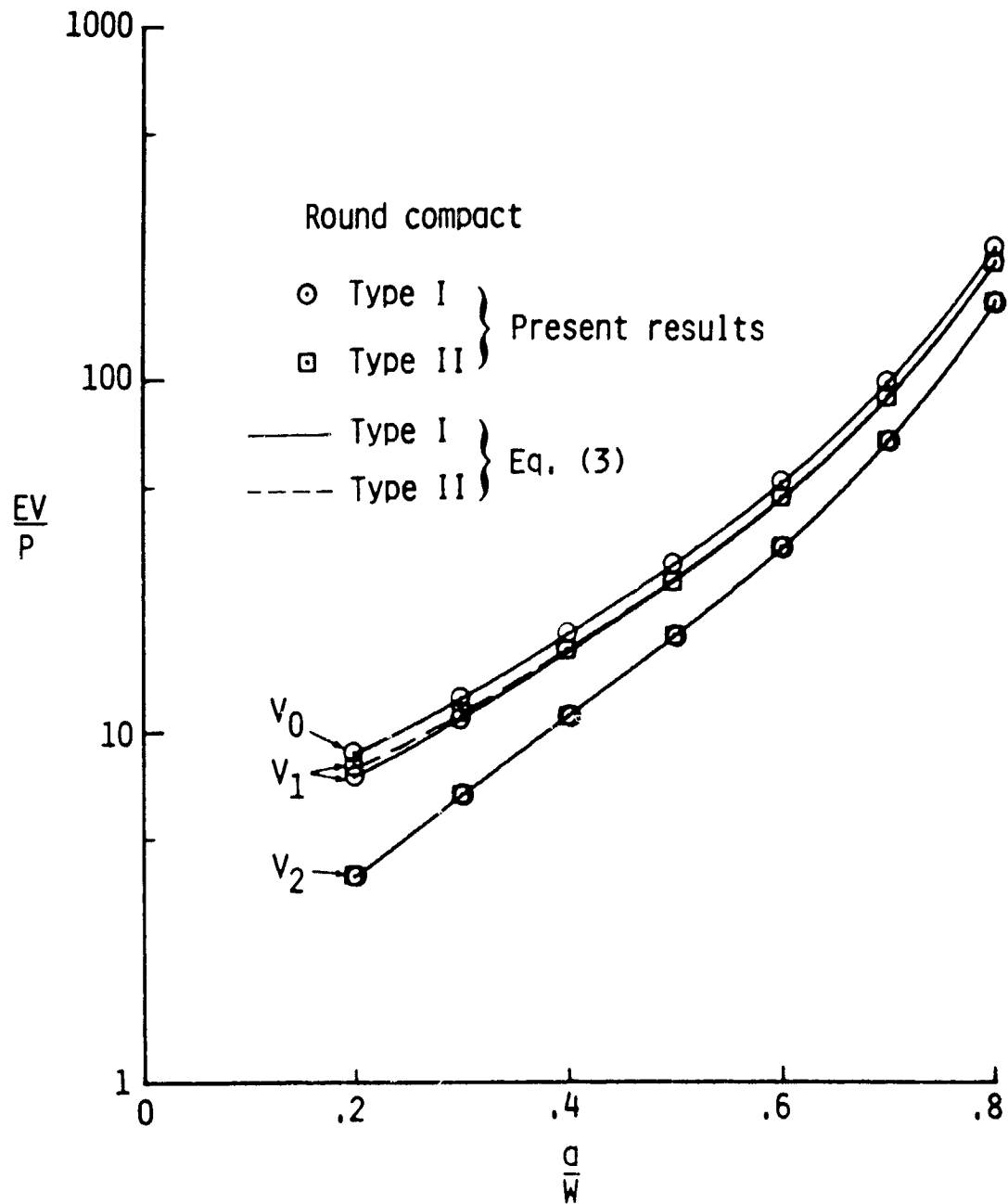


Figure 5.- Normalized crack-surface displacements for round compact specimens as a function of a/W .

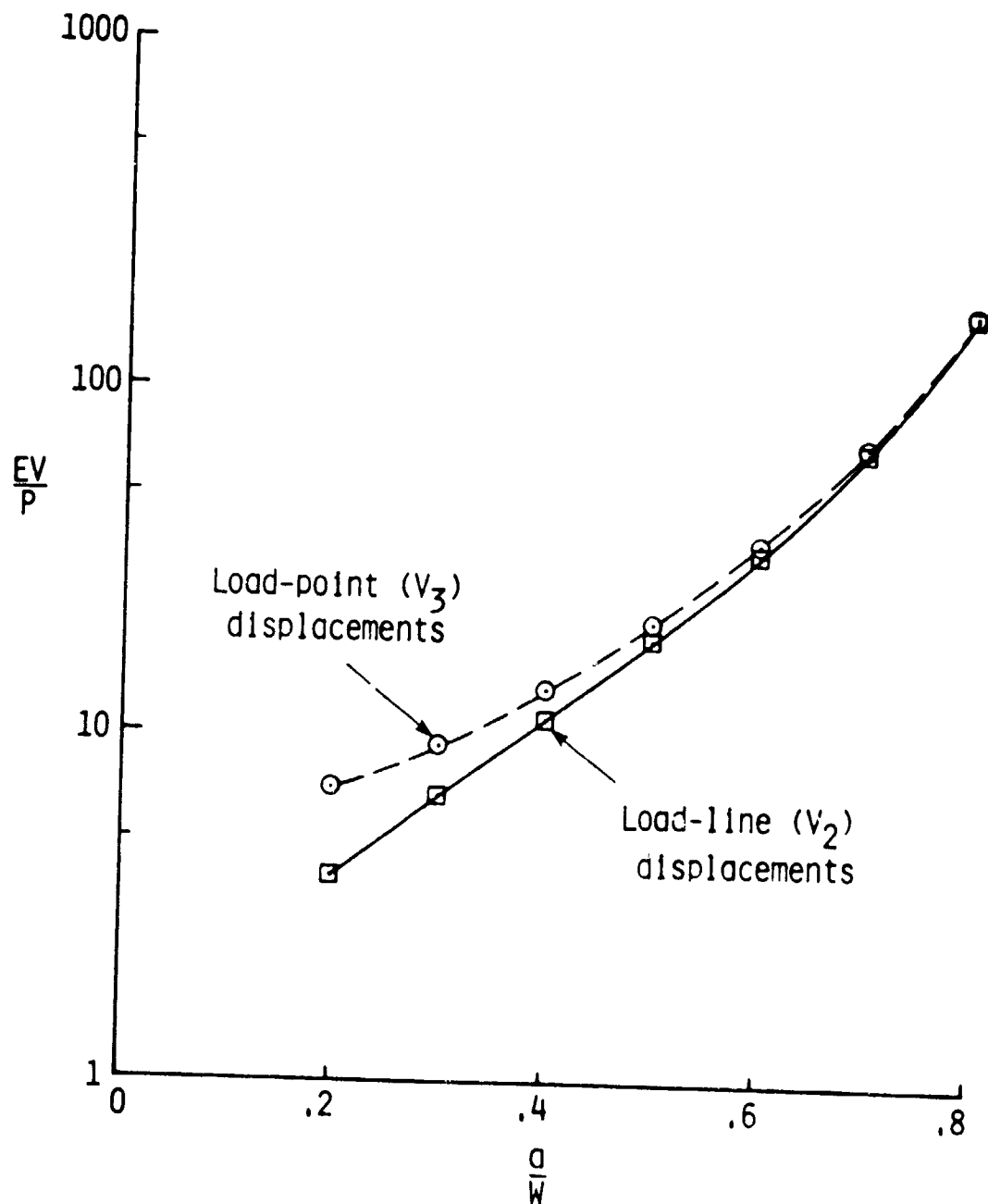


Figure 6.- Normalized load-point and load-line displacements for round compact specimen (type I) as a function of a/W .

1. Report No. NASA TM-80174	2. Government Accession No.	3. Recipient's Catalog No.	
4. Title and Subtitle STRESS-INTENSITY FACTORS AND CRACK-OPENING DISPLACEMENTS FOR ROUND COMPACT SPECIMENS		5. Report Date October 1979	6. Performing Organization Code
		8. Performing Organization Report No.	
7. Author(s) J. C. Newman, Jr.		10. Work Unit No. 506-53-53-01	11. Contract or Grant No.
9. Performing Organization Name and Address NASA Langley Research Center Hampton, VA 23665		13. Type of Report and Period Covered Technical Memorandum	
		14. Sponsoring Agency Code	
12. Sponsoring Agency Name and Address National Aeronautics and Space Administration Washington, DC 20546		15. Supplementary Notes	
16. Abstract A two-dimensional, boundary-collocation stress analysis was used to analyze various round compact specimens. The influence of the round external boundary and of pin-loaded holes on stress-intensity factors and crack-opening displacements was determined as a function of crack-length-to-specimen-width ratios. A wide-range equation for the stress-intensity factors, like that developed for the "standard" rectangular compact specimen, was developed. Equations for crack-surface displacements and load-point displacements were also developed. In addition, stress-intensity factors were calculated from compliance methods to demonstrate that load-displacement records must be made at the loading points and not along the crack line (as is customary) for crack-length-to-specimen-width ratios less than about 0.4.			
17. Key Words (Suggested by Author(s)) Stress analysis Stress-intensity factor Cracks		18. Distribution Statement Unclassified - Unlimited Subject Category 39	
19. Security Classif. (of this report) Unclassified	20. Security Classif. (of this page) Unclassified	21. No. of Pages 26	22. Price* \$4.50